Chapter 6

Development of parameters for use in the model

6.1 Fitting model parameters to knee extension data

6.1.1 Introduction

The muscle model requires a large number of constants to be assumed for each component equation within the model. While many of these constants have been examined under a variety of conditions (eg Hill constants), they have not been confirmed for contractions performed by SCI individuals contracting muscles via NMES. Other constants such as tendon slack length are very dependent upon other aspects of the model and have not been extensively studied to date.

The knee extension experiments from Chapter 5 provide a source of data collected under controlled conditions for the purpose of fitting parameters to the model's equations. This chapter will use the available data to either fit or confirm constants derived from the literature. The isometric data from Section 5.1 were collected for fitting tendon slack length and muscle moment arms to torque generated at different joint angles. In addition, it was planned to derive time constants for the rise and fall of torque in response to stimulation onset and cessation from this isometric data. The isokinetic data from Section 5.2 were collected for the purpose of fitting Hill constants to the torque generated at a single joint angle for each trial. These a-priori fitting procedures are described in Sections 6.1.2 to 6.1.8. The decision to test activation rise rates during dynamic contractions in Section 6.1.9 was taken after the data was collected. For this reason, the data is less well suited to this purpose. Section 6.1.9 has been included, however, as it provides an interesting test of the model under dynamic conditions.

While definite conclusions cannot be drawn due to limitations in the data set, this section provides novel results that deserve more attention in future research.

6.1.2 Fit tendon slack length to isometric data

The purpose of this first section was to select appropriate tendon slack lengths for the model. Slack length is a critical parameter for determining the length-tension relationship of an entire muscle because it determines the length of a fibre for a particular muscle-tendon length. Slack length cannot be measured directly owing to the difficulty in establishing a length without tension on the series elastic component (Hoy et al. 1990). Hoy et al. (1990) estimated slack length by choosing lengths that would produce joint torque curves approximating those measured in-vivo. Any change in a model's fibre length, muscle moment arms or whole muscle-tendon length would alter the model's joint torque-angle curve requiring new slack lengths to be used. If slack lengths are not fitted to a specific model, then modelled joint torque-angle curves will not likely provide a good match to in-vivo measurements (eg Barrett, 1998).

The procedure of Hoy et al. (1990) was used to produce appropriate slack lengths for the present model. This procedure assumes that all knee extension muscles reach their optimum length at the same joint angle. While this is unlikely to be true, muscle force - joint angle curves would be required for each individual muscle to fit separate slack lengths. Meijer et al. (1998a), using a similar model with a single lumped vastus muscle, fitted slack lengths to the rectus femoris and vastus muscle simultaneously without the necessity for both to peak at a common joint angle. While this procedure did improve the fit to experimental data, it has not been adopted here because of concern about the effect of assuming all vastii muscles to be consistent while rectus femoris can differ. While is appears reasonable that rectus femoris may generate peak torque at a different knee angle to the vastii, it seems equally reasonable that individual vastii may also vary. The decision to hold all vastii constant may therefore result in an unreasonable estimate of slack length for the much weaker rectus muscle, to compensate for this assumption. In the absence of further data quantifying force length curves for individual muscles, the present study will assume that all quadriceps muscles peak at a consistent knee angle. This process will be discussed further in Section 6.1.7.

Modelling Methods

Isometric knee extension contractions were modelled using the muscle model described in Section 4.2 with fixed knee angles corresponding to the isometric data presented in Chapter 5. All model parameters except tendon slack length were set to values selected from the literature review (Section 2.4). Tendon slack length was treated as an independent variable rather than a constant. Measured knee extension torques were normalised against Max Torque and compared with the extension torque generated by modelled rectus femoris and vastii muscles at each knee angle. Tendon slack length was adjusted for both muscles to minimise the squared differences between modelled and experimentally measured torques (Figure 6.1.2.1). All minimisation was performed using the FindMinimum function within Mathematica.

Figure 6.1.2.1 illustrates modelled torques by each muscle compared to the experimental data. Modelled extensor torques were well aligned with measured data owing to the fit of tendon length, however the modelled data tended to be slightly less than measured values towards the extreme angles. This result should have been anticipated because, in reality, not all quadriceps muscles would be expected to reach optimum length at the same joint angle. Muscles peaking at different joint angles would widen the active torque-angle curve. With four quadriceps muscles, however, the fitting process would then be indeterminate. The assumption of common peak joint angle for all muscles must be considered a limitation of the present method of fitting tendon slack lengths. Figure 6.1.2.2 shows the pattern of torque produced by vastii and rectus femoris muscles combined.

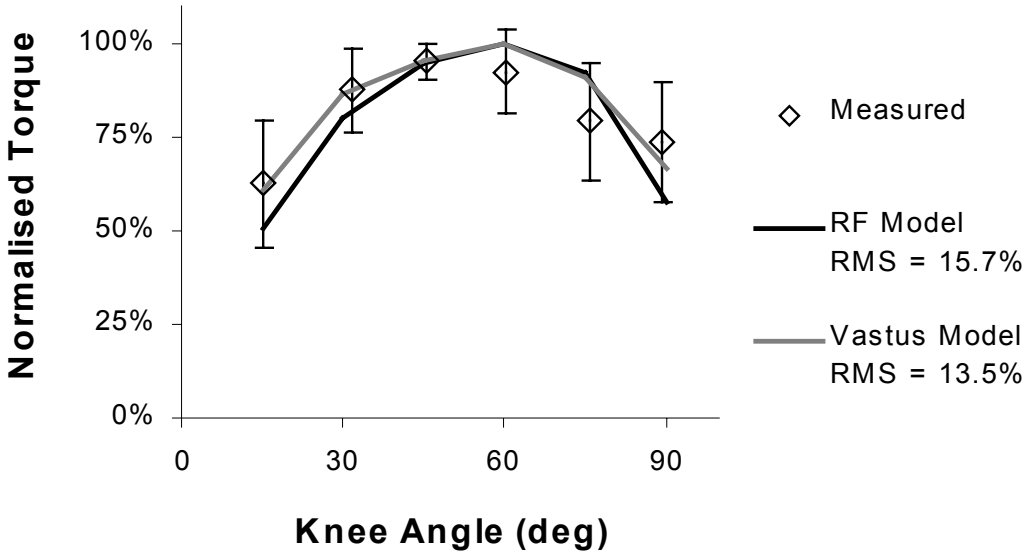

Figure 6.1.2.1 Normalised torque produced by rectus femoris and vastii after fitting tendon slack length

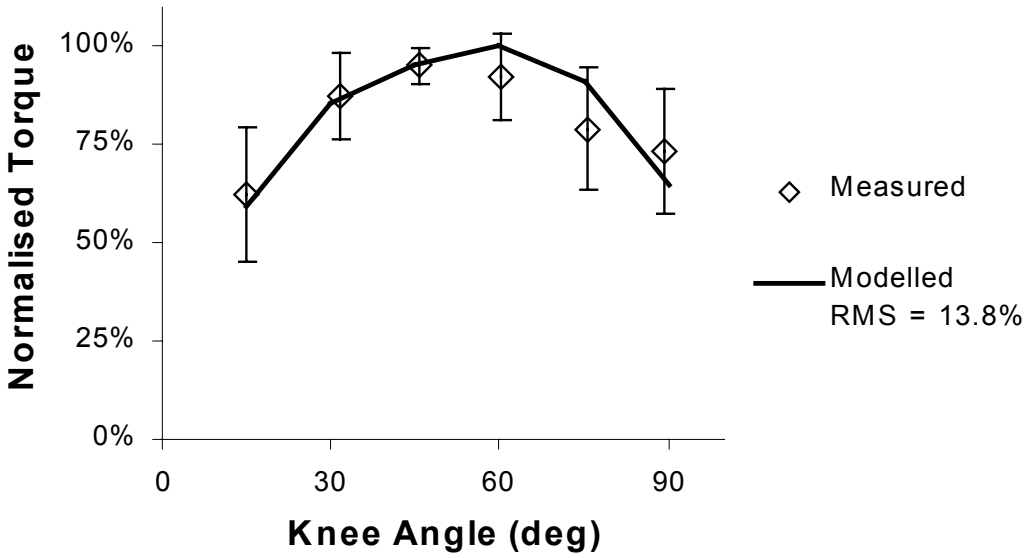

Figure 6.1.2.2 Normalised torque produced by entire quadriceps after fitting tendon slack length

The current fitted rectus femoris tendon lengths were comparable to those fitted by Hoy et al. (1990) (6% difference), however the vastus was 32% smaller (Table 6.1.2.1). The difference in vastus tendon length must be due to a difference in modelled whole muscle tendon length because Hoy and colleagues' slack lengths would result in fibres being shorter than their active range if used in the present model. Hoy et al. did not report a thigh segment length corresponding to their model. If they modelled using a longer segment than the present model, then this would have required a correspondingly longer tendon length since both models used similar fibre lengths. The whole muscle-tendon length would have been expected to be similar because both models used origin and insertion locations based on the data of Brand et al. (1982).

Table 6.1.2.1 Comparison between slack lengths fitted by Hoy et al. (1990) and those fitted within the present section.

	Hoy et al., 1990	Present Study	Difference
Rectus Femoris	0.373 m	0.351 m	-5.9%
Vastii	0.228 m	0.156 m	-31.6%

6.1.3 Low velocity dynamic contractions

The aim of this section was to examine dynamic knee extension torques at low speed in order to test the suitability of the model to dynamic as well as isometric contractions. Only fully active contractions at the lowest velocity were examined in this section in order to test the model's dynamic performance without added complications from activation dynamics or force-velocity effects.

Two measured contractions were selected for each subject from the trial collected at an extension velocity of 10 deg s^{-1}. Only a single contraction was available for one subject because of inconsistent stimulator current during the trial. From each contraction, the fully active portion of the data was visually selected to eliminate activation transients while stimulation was switched on and off.

An isokinetic knee extension model was developed using the previously fitted tendon slack lengths and literature values for all other constants. A separate model was produced for each trial and modelled knee angles were matched to the experimental data. It was necessary to adjust strength levels for each model because of the large differences in muscle force generated by each subject. This was achieved by setting the maximum isometric strength of rectus femoris as an independent variable. For each subject, the modelled knee extension torque was compared to experimental data and rectus femoris isometric strength adjusted to minimise the squared residual error between measured and modelled data. Vastii isometric strength was adjusted automatically within the model by setting vastii strength equal to 5.04 times the rectus femoris strength. This figure was based on the relative cross sectional area of each muscle (see Section 2.4.6). Measured and modelled torques were then normalised against the modelled isometric force of each muscle multiplied by the maximum moment arm. This normalising process allowed for comparison between subjects. After normalising, the modelled torque-angle curves were the same for all subjects.

Figure 6.1.3.1 illustrates the modelled knee extension torque compared to measured data from each subject. Individual subjects display different patterns of joint torque, which may be partially explained by individual tendon slack lengths resulting in a different angle for peak torque. For example, Subject D had limited flexibility and was not able to extend the knee to 15 deg. The curve for this subject demonstrates peak torque occurring at a more flexed position which would be anticipated given his contracture (Figure 6.1.3.1). While a different tendon slack length for each individual would improve the quality of fit, this departs from the original intention to produce a single model predicting behaviour for all subjects.

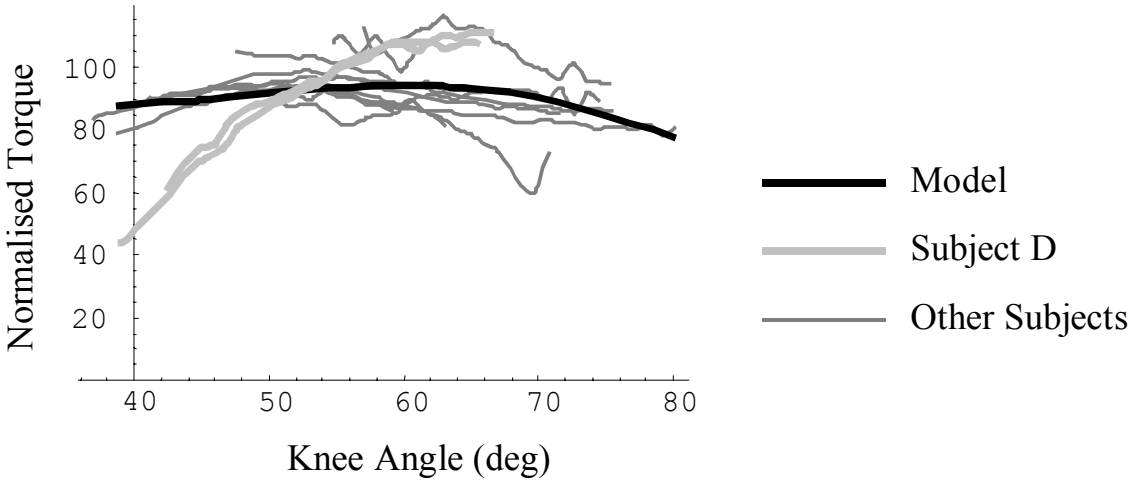

Figure 6.1.3.1 Comparison between knee extension contractions measured from each subject during knee extension contractions at 10 deg s^{-1} and those modelled using the parameters outlined in Section 6.1.2.

6.1.4 Fit both tendon length and moment arms to isometric data

The modelled isometric knee extension torques illustrated by Figure 6.1.2.2 do not exactly coincide with the experimentally measured data. One option for improving the quality of fit was to modify the muscles' moment arm - joint angle relationship. While there were other options available (eg to modify the model's fibre lengths or the sarcomere force-length relationship), moment arms were a likely candidate because of the wide variety of values available from the literature. The purpose of this section was therefore to determine whether modifying the moment arms would improve the degree of fit.

Within the muscle model, the initial moment arm equation of Kellis and Baltzopoulos (1999) was replaced by a quadratic equation of the form:

$$Drfk(\theta_k) = a + b\,\theta_k + c\,\theta_k^2$$

Equation 6.1.4.1

where a, b and c were constants. Altering a muscle's moment arm will affect its tendon length; hence five independent variables were used for this section, the three moment arm constants and tendon slack lengths for the two extensor muscles. These five variables were then fitted

according to the method outlined in Section 6.1.2 to minimise differences between the modelled and experimentally measured torques for the rectus femoris and vastii muscles. Again, separate residual errors were produced for each muscle with the assumption that both muscles produced torque curves matching the total joint torque curve.

Fitting moment arm as well as slack length made little difference to the overall quality of fit (Figure 6.1.4.1). This was to be expected since the original fit was very close. Fitted moment arms were reduced slightly but remained similar to those of Kellis and Baltzopoulos (Figure 6.1.4.2). The fitted tendon lengths displayed in Table 6.1.4.1 were not very different from those fitted in Section 6.1.2.

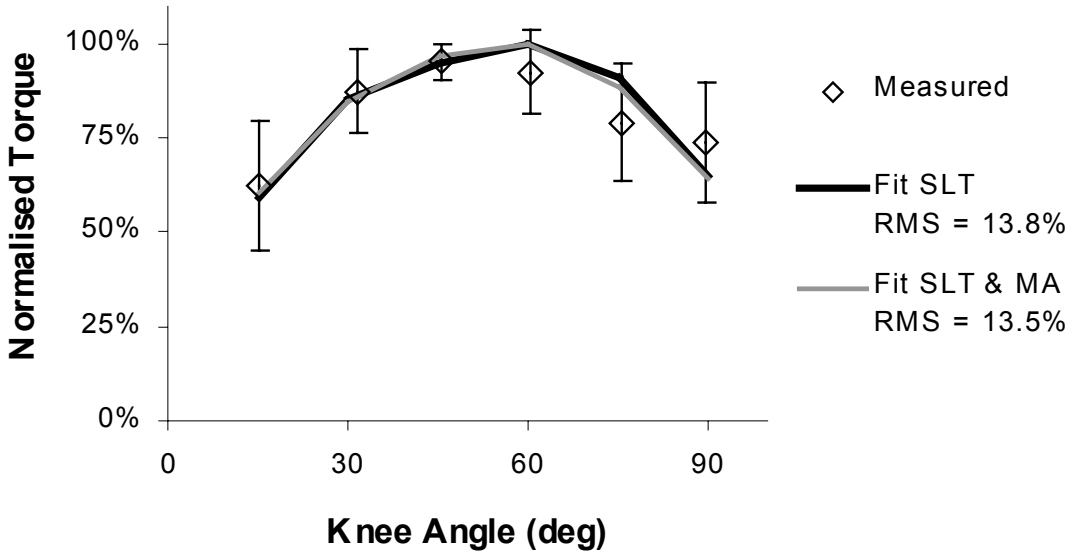

Figure 6.1.4.1 Comparison between measured isometric joint torques, those modelled by fitting just tendon lengths from Section 6.1.2 and those modelled by fitting moment arms as well as tendon lengths.

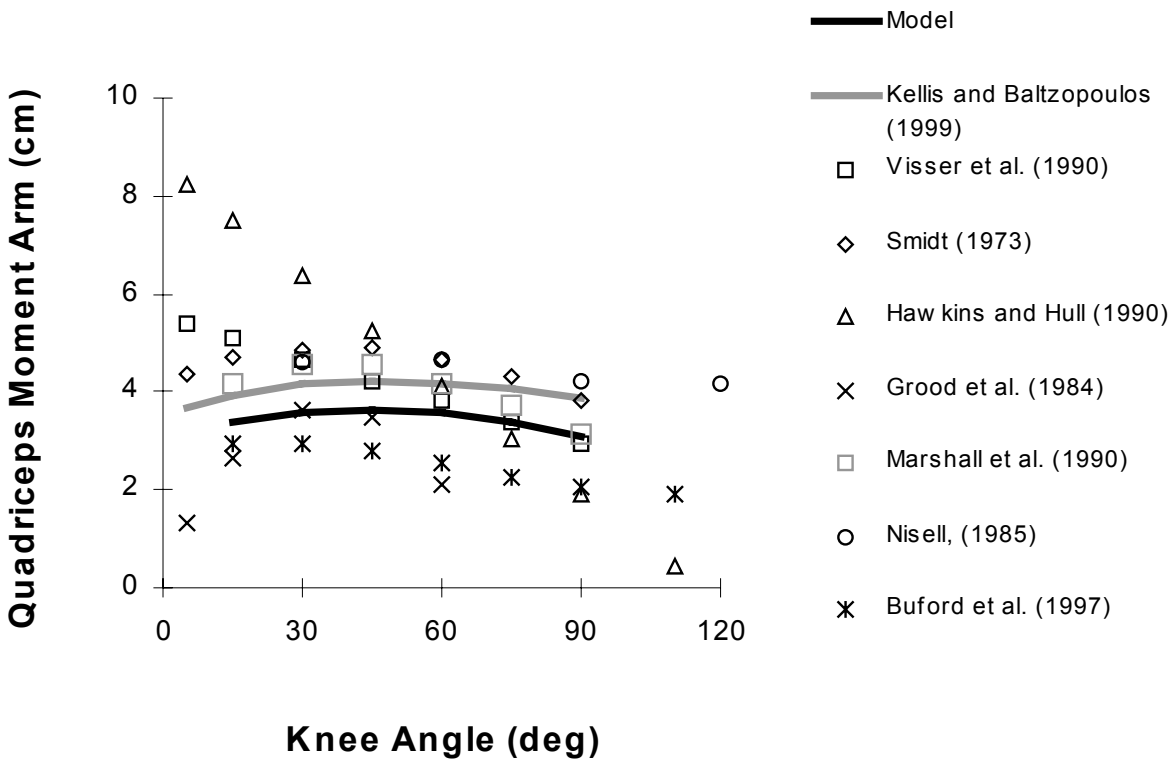

Figure 6.1.4.2 Comparison between moment arms derived from a number of published sources and those fitted to match isometric data.

Table 6.1.4.1 Comparison between slack lengths fitted by Hoy et al. (1990) and those fitted using two different quadriceps moment arms across the knee.

	Fitted to moment arms of Kellis and Baltzopoulos	Moment arms and tendon lengths both fitted	Difference
Rectus Femoris	0.351 m	0.345 m	-1.7%
Vastii	0.156 m	0.152 m	-2.6%

Fitting moment arms as well as tendon lengths only decreased the residual error from an RMS of 13.8% for Kellis and Baltzopoulos' moment arms to an RMS of 13.5%. The significance of this improvement was assessed using a single tailed T-test for paired means on the squared

residual error between measured and modelled values, with and without moment arm fitting. Fitting a new moment arm equation did not produce a significantly improved fit to the data ($p>0.31$). Therefore, there is no justification from this process to use moment arms other than those measured experimentally by Kellis and Baltzopoulos (1999).

6.1.5 Dynamic contractions at different velocities

There is substantial variation in the range of Hill constants that have been measured experimentally (Section 2.4.6). Furthermore, it could be expected that spinal cord injury may alter the dynamic properties of skeletal muscle in ways not completely understood. Therefore, the purpose of this section was to compare isokinetic contractions at different velocities to test the suitability of the chosen Hill constants.

It could have been possible to test entire contractions in a fashion similar to Section 6.1.3. This procedure was not carried out, however, owing to the large and variable number of trials involved. It is difficult to distinguish lack of fit caused by unsuitable Hill constants from lack of fit caused by other factors like tendon slack length (eg Figure 6.1.3.1). Furthermore, the large amount of data involved with whole trials would have prevented the fitting of new constants that was planned for Section 6.1.6. Fitting two trials to seven subjects across seven different velocities would have required 98 different simulations to be included within the one minimisation function with nine different variables to be simultaneously optimised (Hill constants a and b as well as isometric strength for the seven subjects). Such a fitting procedure was not practical. Therefore, for the dual reasons of data presentation and ability to perform parameter fitting, the decision was taken to analyse data only at the discrete knee angle of 60 deg.

During the isokinetic experiments, each subject completed three or four contractions at each extension velocity. Nett torque was averaged over the period when the knee angle was between 60.5 and 59.5 deg for each contraction. Stimulation had to be active for a period of at least 100 ms prior to reaching 60 deg in order for a trial to be included. This ensured that the muscles were maximally activated at the time of recording. Nett torque at 60 deg was averaged across three contractions for each subject at each knee extension velocity. Data points were discarded if the stimulation current differed by more than 7% from the average current recorded during the isometric trials. Table 6.1.5.1 gives the mean and standard

deviation of torques recorded for each subject. These data were subsequently normalised as a percentage of isometric torque prior to comparison with the model output.

Table 6.1.5.1 Knee extension torques measured at a knee angle of 60 deg for all subjects at each velocity of knee extension.

Velocity (deg s^{-1})	Subjects						
	A	B	C	D	E	F	G
0	11.1 (100%)	20.4 (100%)	18.6 (100%)	17.5 (100%)	12.5 (100%)	13.7 (100%)	15.9 (100%)
10		22.9 (113%)	18.8 (101%)	13.8 (78%)	14.4 (115%)	12.0 (87%)	15.1 (95%)
30	9.7 (88%)	19.3 (95%)	17.5 (94%)	15.5 (89%)	12.5 (100%)	12.2 (89%)	
60	9.5 (86%)	14.5 (71%)	14.2 (76%)	13.8 (79%)	12.4 (99%)	10.2 (74%)	
90		16.1 (79%)	11.6 (62%)	13.2 (75%)	10.9 (88%)	10.4 (75%)	
120		16.3 (80%)	9.6 (52%)	11.1 (63%)		7.4 (54%)	
240		7.4 (36%)	5.2 (28%)	7.7 (44%)	5.0 (40%)	5.3 (38%)	5.5 (35%)

Data represent gravity corrected torques in N m followed by normalised (% isometric) torques in brackets.

Missing values were discarded when stimulation currents differed by more than 7% from the reference levels.

One isometric and six isokinetic contractions were modelled, one for each experimentally recorded velocity of contraction. Isokinetic simulations were performed through a complete knee extension from 90 deg with the quadriceps fully active throughout and the torque at 60 deg recorded for comparison with experimental data. All data were normalised as a percentage of isometric torque prior to comparison. For this reason, there was no need to run separate simulations for each subject.

Figure 6.1.5.1 illustrates the comparison between measured and modelled results. While there is some variance between subjects in the amount of torque decline with increasing velocity, the modelled values fit well within the range of experimental results. The current values for Hill's constants therefore seem appropriate for modelling NMES contractions performed by SCI individuals. The following section will provide a statistical test of this statement by attempting to improve the model's fit to experimental data.

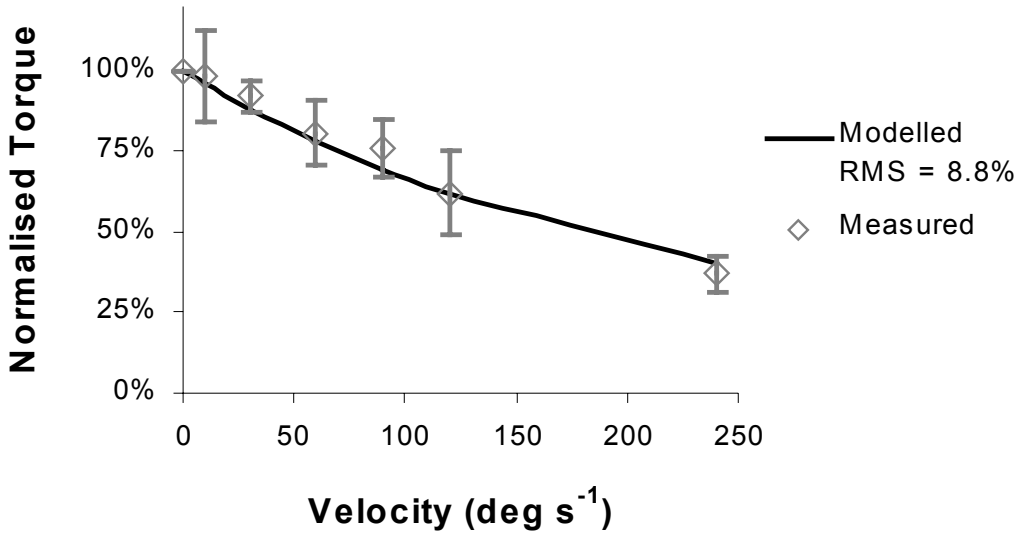

Figure 6.1.5.1 Comparison between torques measured at 60 deg knee flexion for all subjects at each velocity of knee extension and those modelled using Hill constants chosen from published literature .

6.1.6 Fit Hill constants to dynamic contractions

It was decided a-priori to fit new Hill constants to the available experimental data because of the range of constants used in various modelling sources (Section 2.4.4). Whilst it appears from Section 6.1.5 that this process was not required, it was still performed in order to statistically demonstrate the suitability of the chosen constants.

The simulations from Section 6.1.5 were repeated, setting Hill constants a and b as independent variables. Similarly to previous sections, modelled knee extension torques were compared to experimental data and the Hill constants adjusted to minimise the squared residual error between measured and modelled data. Table 6.1.6.1 demonstrates the change in Hill constants with data fitting and their effect on modelled torques. Fitting new Hill constants only reduced the RMS error from 8.81% down to 8.76%, the variability thus being due to experimental variation, not lack of fit to the model. A single tailed T-test for paired means indicated that fitting new constants did not significantly reduce the mean squared residual error ($p>0.3$). Therefore, the original Hill constants chosen from literature sources will continue to be used in subsequent modelling processes.

Table 6.1.6.1 Comparison between Hill constants fitted within the present study to those reported in previous literature.

	Constant a	Constant b
Values chosen from literature (Pierrynowski and Morrison, 1985)	0.35 × isometric force	2.25 × fibre length
Fitted in present study	0.351 × isometric force	2.250 × fibre length

6.1.7 Discussion of interaction between variables

Parameters used in a model are often interrelated in manners than may not be expected. This limits the suitability of fitting constants to in-vivo data, as there are often multiple solutions to improving the fit of data. This section will serve to illustrate some of those inter-dependencies and highlight cautions that should be used when fitting data.

This chapter has used the dimensionless fibre force-length equation described by Delp et al. (1990) and made available by the International Society of Biomechanics (http://isb.ri.ccf.org/data/delp). There are, of course, alternative ways to model this relationship and these have been described in Chapter 3). The force-length equation of a single sarcomere from Section 3.2 generated a curve of similar shape to that of Delp et al. (1990), but produced less active force at lengths below resting (Figure 6.1.7.1)

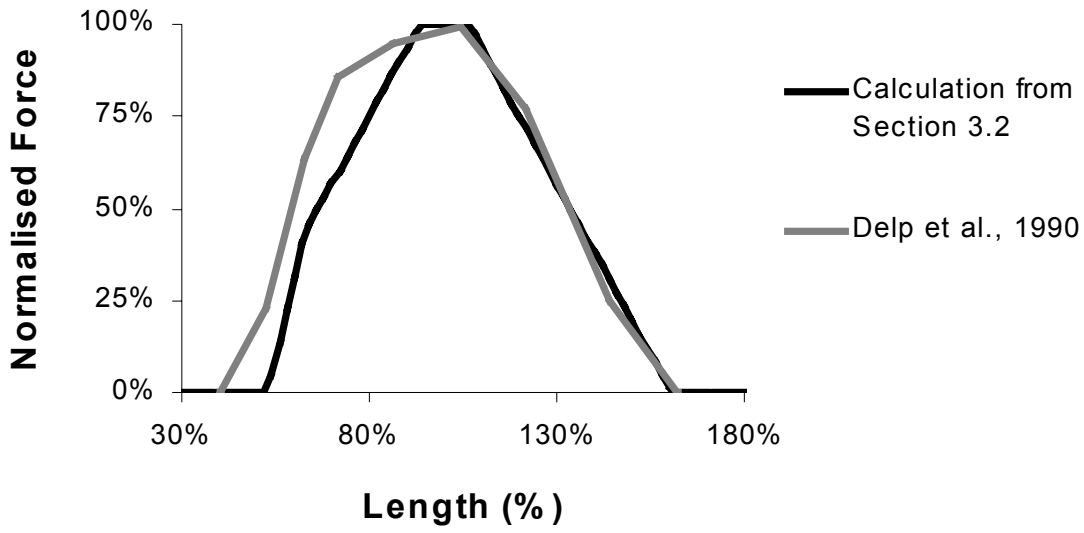

Figure 6.1.7.1 Comparison between the force length curve described by Delp et al. (1990) and that calculated for a single human sarcomere in Section 3.2.

When the single sarcomere equation from Section 3.2 was used in the methods of Section 6.1.2, the model predicted that torque would be reduced at extreme joint angles (Figure 6.1.7.2).

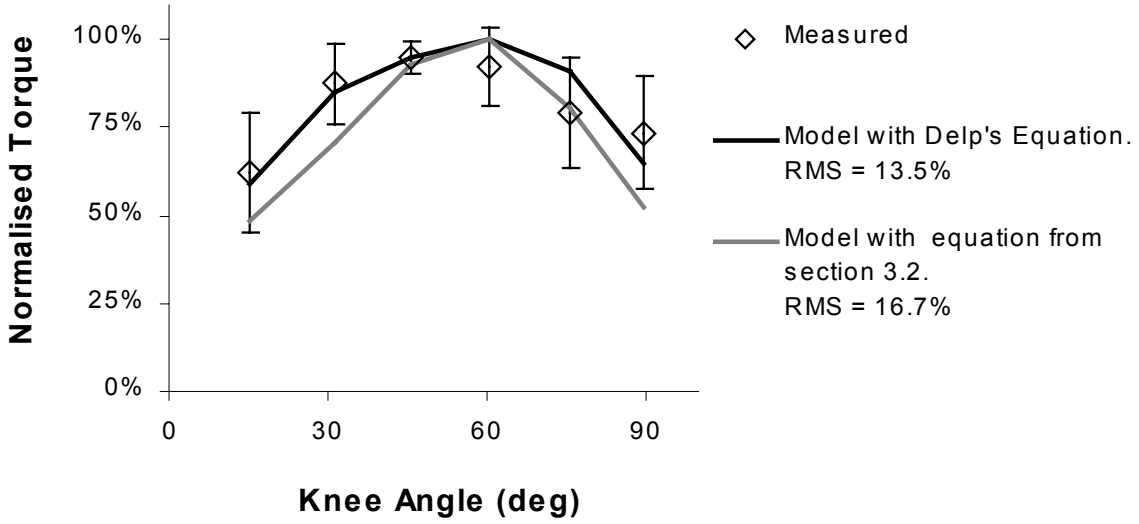

Figure 6.1.7.2 Comparison between measured isometric joint torques and those modelled using the two different force-length equations illustrated in Figure 6.1.7.1 .

Decreasing the model's quadriceps moment arm could widen the torque-angle curve by reducing the amount of muscle length change for a given range of joint angles. Using the methods described in Section 6.1.3, a new moment arm-angle equation was produced and the results of this fitting process can be seen in Figures 6.1.7.3 and 6.1.7.4.

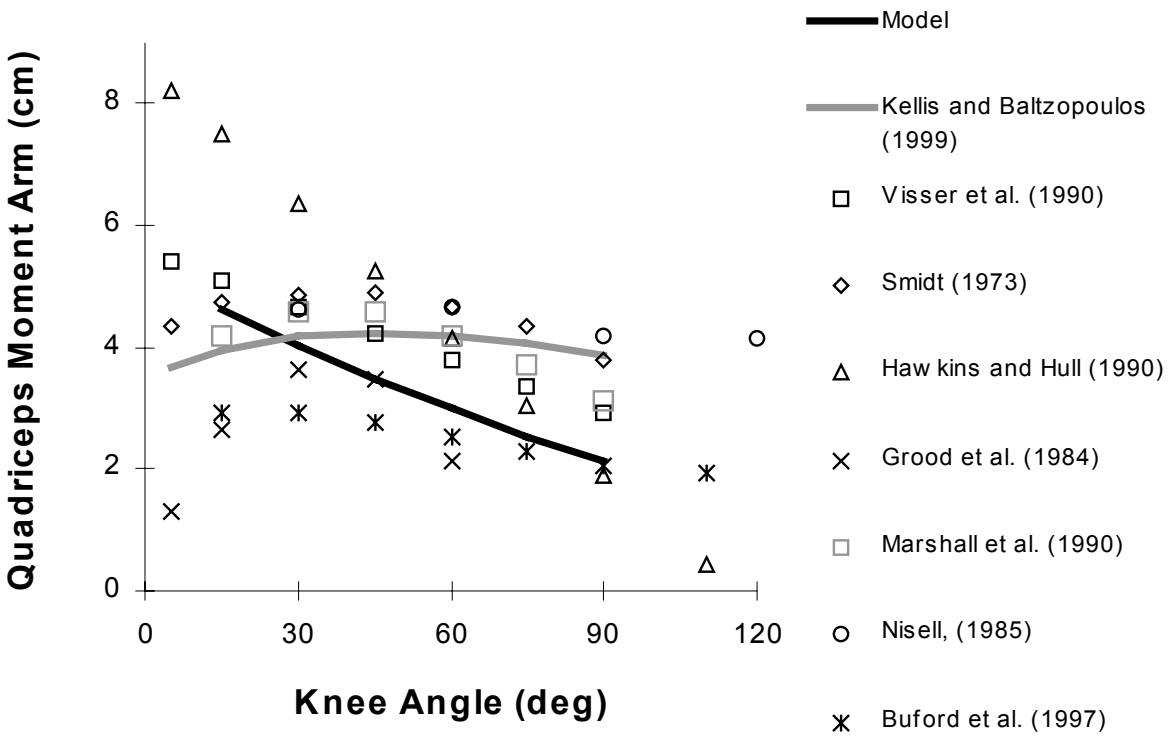

Figure 6.1.7.3 Comparison between quadriceps moment arms from multiple literature sources and those determined by fitting the model to experimental data using the human sarcomere force-length relationship.

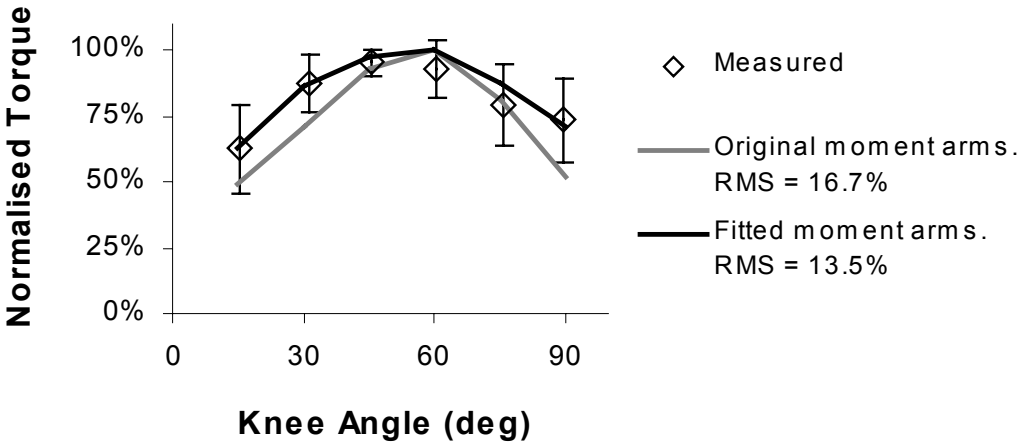

Figure 6.1.7.4 Comparison between experimentally measured isometric torques and those produced by modelling. Both modelled curves use the human sarcomere force-length relationship from Section 3.2. The grey curve uses original moment arms from Kellis and Baltzopoulos (1999) while the black curve uses new moment arms fitted to match the data.

This initially looked like a satisfactory solution. The fit between measured and modelled data was very good and the new moment arm-angle relationship was within the bounds of values available from the literature. Indeed, the linear shape of the relationship was quite similar to that found by Visser et al. (1990).

Problems with this fitting procedure only became apparent later when investigating Hill constants during dynamic contractions. Notice in Figure 6.1.7.4 that, at 60 deg, the moment arms produced by the fitting routine are smaller than those found by all of the reported studies except for Buford et al. (1997) and Grood et al. (1984). A smaller moment arm requires that, for a given angular velocity of the knee, the linear velocity of shortening for the muscle must be less. Using smaller moment arms therefore meant that the model predicted a smaller decline in torque with increasing angular velocity (Figure 6.1.7.5). To correct this problem and accurately model dynamic contractions meant that different Hill constants would be required. In fact, to correct the model as shown in Figure 6.1.7.5, Hill's constant a had to be increased from 0.35 up to 0.55. This was outside the ranges of values commonly reported in literature (Baratta et al., 1995, Fitts et al. 1991).

Table 6.1.7.1 Changes in Hill constants with fitting procedure.

	Constant a	Constant b
Literature values (Pierrynowski and Morrison, 1985)	0.35 × isometric force	2.25 × fibre length
Fit constants using Delp's force-velocity relationship	0.351 × isometric force	2.250 × fibre length
Fit constants using the single sarcomere equation from Section 3.2	0.550 × isometric force	1.905 × fibre length

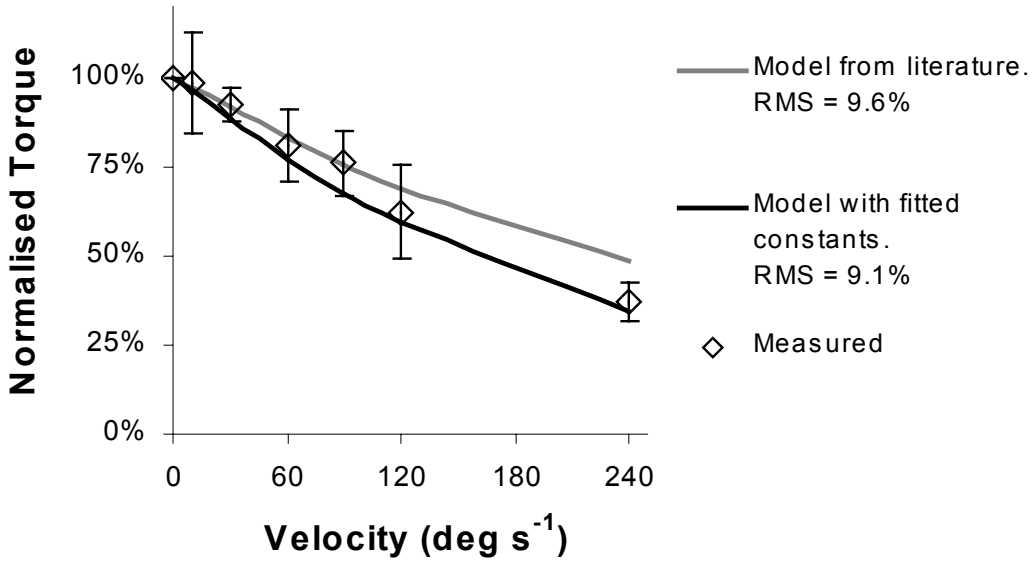

Figure 6.1.7.5 The effect of fitting Hill constants on modelled torque-velocity relationship when using the human sarcomere force-length relationship.

The above discussion demonstrates that fitting constants to one part of a model may have unexpected consequences on other parts of the model. For example, the use of a different force - length relationship could be accommodated by altering the moment arm - joint angle equation. Changing the moment arms was successful in the immediate task of fitting isometric

torques at different knee angles, but had deleterious effects on the model's performance during dynamic contractions.

There were alternative solutions to fit the measured isometric torques. For example, optimum fibre length could have been increased as longer fibres generate force over a greater length (Lieber, 1992). Alternatively, the optimum length of individual quadricep muscles could have been set to occur at different knee angles or the fibre force-length relationship altered. Just because changing moment arms resulted in an excellent fit doesn't mean that this option was the best available.

The interaction between parameters such as moment arm, fibre length and tendon length has been highlighted by Meijer et al. (1998a). Individuals with unusually large moment arms would be expected to have correspondingly long fibre lengths in order to achieve active force over similar ranges of joint angle. When different parameters are derived from different sources, this co-variance may be missed.

Meijer et al. (1998a) found that a simple model using parameters that were all measured from the same four subjects gave the best fit to voluntary isometric knee extension torque-angle curves. They concluded that this was due to using parameters sourced from a single population so co-variance of parameters was taken into account. Unfortunately, not all components of the model could be measured from cadavers, and this may have affected the conclusions of Meijer et al. The parameter showing the greatest difference between values estimated from literature and measured by Meijer et al. was vastii fibre length (they used a single lumped vastus model similar to the present model). Meijer et al.'s vastus fibre length was 11.3 cm; significantly longer than is commonly reported in the literature (Section 2.4.4). At the same time, Meijer et al. used the force-length equation of Out et al. (1996), which obviously they could not measure directly from their study. Had they used a wider force-length relationship (eg Delp et al., 1990) they might have concluded that the literature parameters provided a better fit. Alternately, had they used three separate vastii and allowed them to reach maximum torque at different knee angles, this would also have improved the fit of their literature value parameter model to be indistinguishable from their measured parameter models.

When a model doesn't fit the observed data, it is impossible to determine exactly which parameters are responsible because of the interdependent nature of the parameters. While Meijer et al. (1998a) demonstrate that measuring all parameters from the one source improved the fit for their data, they cannot be sure that this was the best solution. When developing a model to apply to a range of individuals, it is difficult to justify the use of parameters measured from only a small number of subjects (eg Meijer et al., 1998a). This is particularly so when some of the parameters (eg vastus fibre length from Meijer et al.) are considerably different to those commonly reported in other literature.

6.1.8 Fit activation constants to isometric data.

The purpose of this section was to fit activation time constants to data collected under isometric conditions. Data for the fitting process were taken from isometric contractions collected during the same testing session as the dynamic data (Section 5.2.2), rather than from the more extensive data set of Section 5.1. This decision was taken primarily because it was then easier to compare contractions under both isometric and dynamic conditions. Taking isometric data from the same session as the dynamic data ensured that electrode placements and current levels remained constant, so that the only difference between isometric and dynamic data was the speed of movement.

Four sets of isometric trials were collected at 60 deg knee flexion; evenly spaced before, after and between dynamic trials. The trial producing torque closest to the average across the four isometric trials was chosen for curve fitting. This was the second trial for all but one subject where the third trial was chosen. The average decline in isometric torque was about 21% between the first and last contractions, indicating that fatigue was ongoing despite the rest periods. While Section 5.1.2 indicates that delay constants and rise time were not significantly affected by fatigue, the time for torque to fall after stimulation ceased did increase as muscles fatigued. The average magnitude of torque decline during the dynamic sessions was much less than that measured during the isometric sessions (Section 5.1.2), suggesting that the corresponding fall time changes would also be relatively small. Regardless, the order of knee extension velocities was randomised in order to minimise the effect of this fatigue. Additional variability, however, may have been added to the current results by the presence of progressive fatigue.

Each trial was normalised to 100% of Nett Torque, calculated according to the methods outlined in Section 5.1.2. Although data was originally collected at 1000 Hz, these were re-sampled at 100 Hz in order to minimise the number of data points required for fitting.

During each isometric trial, subjects performed three contractions lasting 2 s, with 2 s rest between contractions. The second and third contractions were selected from the chosen trial for fitting because the first contraction usually had a slower rise rate than the subsequent two. An example from one subject is illustrated in Figure 6.1.8.1. This effect is likely to represent post-tetanic potentiation of the second and third contractions (Partridge and Benton, 1981). It is also possible that there is a mechanical effect arising from changes to compliance within the dynamometer or subjects.

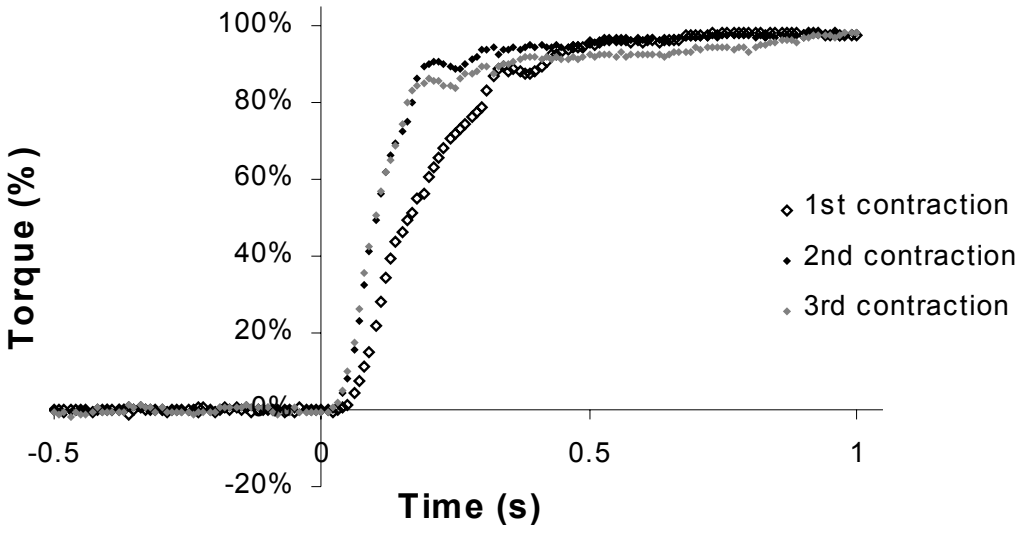

Figure 6.1.8.1 The rise in knee extension torque in response to stimulation onset during three successive isometric contractions by a single subject.

Results from Section 5.1.1 demonstrated that activation timing changed as a function of knee angle. The changes were greatest, however, at angles less than 60 deg with little change for angles greater than this. Quadriceps activation during the isokinetic trials always takes place at angles greater than 60 deg. Similarly, during the cycling experiments described in Chapter 7, stimulation always commenced at knee angles greater than 65 deg and was usually closer to

90 deg. Therefore, in order to simplify the present model, activation timing constants were not adjusted when stimulation commenced at different joint angles.

The activation equation used by Pandy et al. (1990) was modified to include a delay between stimulation onset and force rise. Thus, the activation equation became:

$$\frac{d\,a(t)}{d\,t} = \text{If } u(t - \text{delay}) = 1,$$

$$\text{Then } \frac{1 - a}{\tau_{rise}},$$

$$\text{Else } \frac{a_{min} - a}{\tau_{fall}}$$

Equation 6.1.8.1

In order to allow a different delay for stimulation onset and cessation, a further conditional statement was added so that the Rise Delay constant was used in Equation 6.1.8.1 if time was less than mid-way between stimulation onset and cessation. The Fall Delay constant was used if time was past mid-way. The fitting process was conducted separately for the rise and fall of torque in response to stimulation for the two representative contractions from each subject. This gave a total of 14 contractions used to fit the activation constants.

Stimulation onset

Data from rises in torque after stimulation commenced were normalised as a percentage of Nett Torque prior to fitting. Each contraction was also time normalised so that stimulation commenced at time zero and data from 0.5 s before stimulation to 1 s after stimulation used for fitting (eg Figure 6.1.8.1).

Isometric knee extension contractions were modelled at 60 deg with stimulation commencing at time zero. Literature values were used for all constants except tendon slack length as described in preceding sections. Rise Delay and Rise Time were set as independent variables

for the optimisation. Once again, the squared differences between modelled and experimentally determined torques were minimised to find optimum values of the independent variables. The resulting Rise Delay and Rise Time constants were 53 ms and 48 ms respectively. A comparison of the resulting model and the 14 experimentally measured contractions is shown in Figure 6.1.8.2.

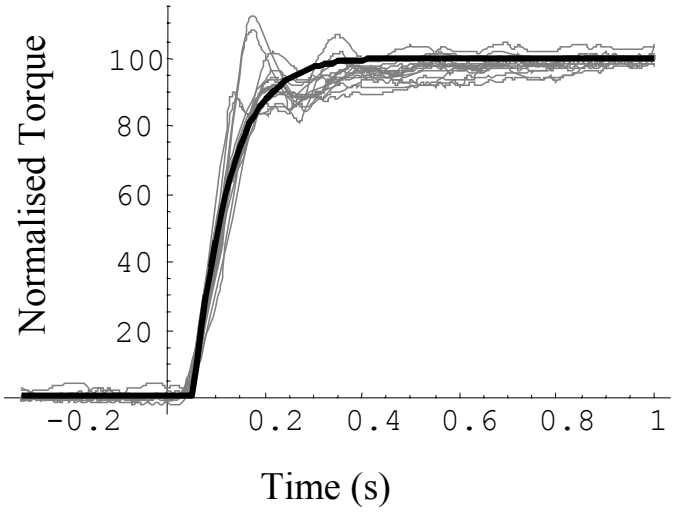

Figure 6.1.8.2 The rise in knee extension torque in response to stimulation onset. Comparison between the modelled rise and all measured data.

It can be seen that the individual trials are remarkably similar, especially during the first part of the rise. Individual responses become more variable towards the plateau of the curve. Note that the plateau is not horizontal, thus the curve cannot be expected to fit perfectly. In practice, the model underestimates the data slightly near the edge of the plateau around 0.2 s but is satisfactory during the rise where the fit of the model is most important. The rising plateau does have implications when comparing isometric with dynamic contractions. This will be discussed later in Section 6.1.9.

There is a dampened oscillating pattern evident in Figure 6.1.8.2. The dampening of this oscillation suggests a compliance effect within the ergometer; either the arm of the ergometer or the padding between the subject and the arm. While this padding was reduced from that recommended by the manufacturer, it could not be eliminated entirely because of the poor blood supply to the skin of SCI individuals. An alternative reason for the torque oscillation

may have been incomplete tetanisation of the muscles being stimulated at a frequency of 35 Hz. This explanation seems less likely because NMES is generally considered to produce full tetanisation at frequencies greater than 30 Hz (Katz et al., 1987).

Stimulation Cessation

Data from falls in torque after stimulation ceased were normalised as a percentage of the torque recorded at the time stimulation ceased. Each contraction was time normalised so that stimulation ceased at time zero and data from 0.5 s before cessation to 1 s after were used for fitting.

Once again, the curve fitting process was able to provide a very good match to measured data, particularly during the first half of torque decline, with resulting constants for Fall Delay and Fall Time being 66 ms and 48 ms respectively. Variability between subjects increased as torque declined below 50%, however the model still split the range of results quite well (Figure 6.1.8.3).

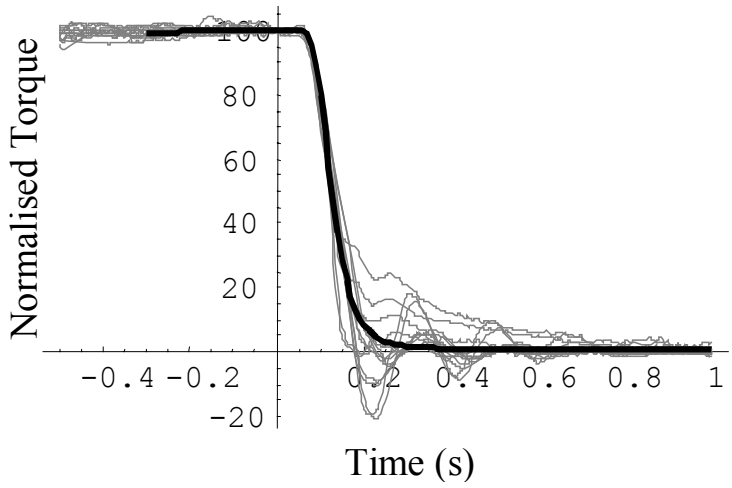

Figure 6.1.8.3 The fall in knee extension torque in response to stimulation cessation. Comparison between the modelled fall and all measured data.

6.1.9 Test activation constants during dynamic contractions.

Limitations of this section

The results of this section cannot be adequately assessed without considering the original aims of the experiment. The dynamic data was collected with the aim of testing Hill constants as per Section 6.1.6. It was therefore not considered important to control the timing of muscle activation, other than to ensure that the muscle had been stimulated long enough to be considered fully active when the 60 deg angle was reached. Stimulation for each trial was triggered manually and therefore happened at a slightly different angle for each trial, often during the periods of high acceleration between knee flexion and the subsequent extension.

When comparing results between contractions, the rate of rise is affected by the muscle length (and hence final maximum force) as well as by the level of activation. A well controlled experiment would have each contraction commencing at the same angle so that this variable is eliminated. While this would now be much easier to perform using software such as Labview, this was not readily available at the time of testing. Furthermore, a new stimulator interface would have been required to enable computer triggering of the stimulation. Finally, and most significantly, if contractions at all velocities had commenced at the same angle (eg 80 deg), then the original aim would not have been realised. If stimulation had not commenced before the knee began extending for high velocity conditions, then full activation would not have been achieved before the angle of 60 deg was reached. This would have precluded the fitting of Hill constants in Sections 6.1.5 and 6.1.6, as well as reducing the range of data available for Sections 6.1.3 and 6.1.4.

The manual stimulation initiation has meant that activation periods were not available for analysis at all velocities for all subjects. For many trials, the rise in muscle force occurred before the target angular velocity was reached; particularly at higher extension velocities. While rise periods were available from all subjects at 30 deg s^{-1}, only three subjects were represented at 90 deg s^{-1}. At 120 deg s^{-1}, only two subjects' data were available and one of those subjects was not represented at 90 deg s^{-1}. Table 6.1.9.1 gives the number of rise periods available for analysis at each contraction velocity. Any statistical analysis of these data is meaningless because of the small numbers and different subjects available at each velocity. The samples at each velocity were neither independent nor repeated measures. Statistical differences between velocities may therefore have resulted from comparing different subjects'

data at each velocity; as well as because of differences caused by the velocity changes. A description of various methods used to analyse the data will be given here, together with a visual interpretation of results.

Table 6.1.9.1 Number of rise periods available for analysis at each velocity of knee extension.

Velocity (deg s^{-1})	Number of Contractions	Number of subjects
0	14	7
10	10	6
30	12	7
60	10	6
90	4	3
120	3	2
240	0	0

Processes attempted comparing activation times at different velocities.

In order to account for the variation in joint angle where each contraction commenced, the rise and fall phases of each trial were normalised as a percentage of maximum torque. To estimate the variation in 100% torque with joint angle, a quadratic curve was fitted to the portions each trial where activation appeared to be maximal. These fully active regions could only be estimated visually because, if a conservative estimate of the time for full activation was used, there would not have been enough data in many trials to fit a curve. Furthermore, a larger amount of extrapolation outside of the fitted region would have been required in order to analyse the rise and fall of muscle activation.

Figure 6.1.9.1 illustrates the normalising process for one trial. Part a shows the quadratic curve fitted to the fully active portions of three successive contractions. The rise and fall

periods were not considered during the curve fitting process; only the thicker traces lying along the quadratic curve. Parts b and c show the activation rise and falls respectively, normalised using the quadratic curve from part a with stimulation onset at time zero. Note that rise and fall periods were discarded if angular velocity was not constant during these times. Therefore, for the trial of three contractions illustrated in Figure 6.1.9.1, only one fall period and two incomplete rise periods were available for subsequent analysis.

There were apparent limitations to this normalising process. For example, on Figure 6.1.9.1, the one contraction with available fall data for this subject normalised to less than 100% at the time stimulation first ceased. Furthermore, neither of the available rise periods extend back to the onset of stimulation. The normalised data did look reasonable, however, and allowed for comparison between subjects differing in strength of contraction and angle of stimulation onset.

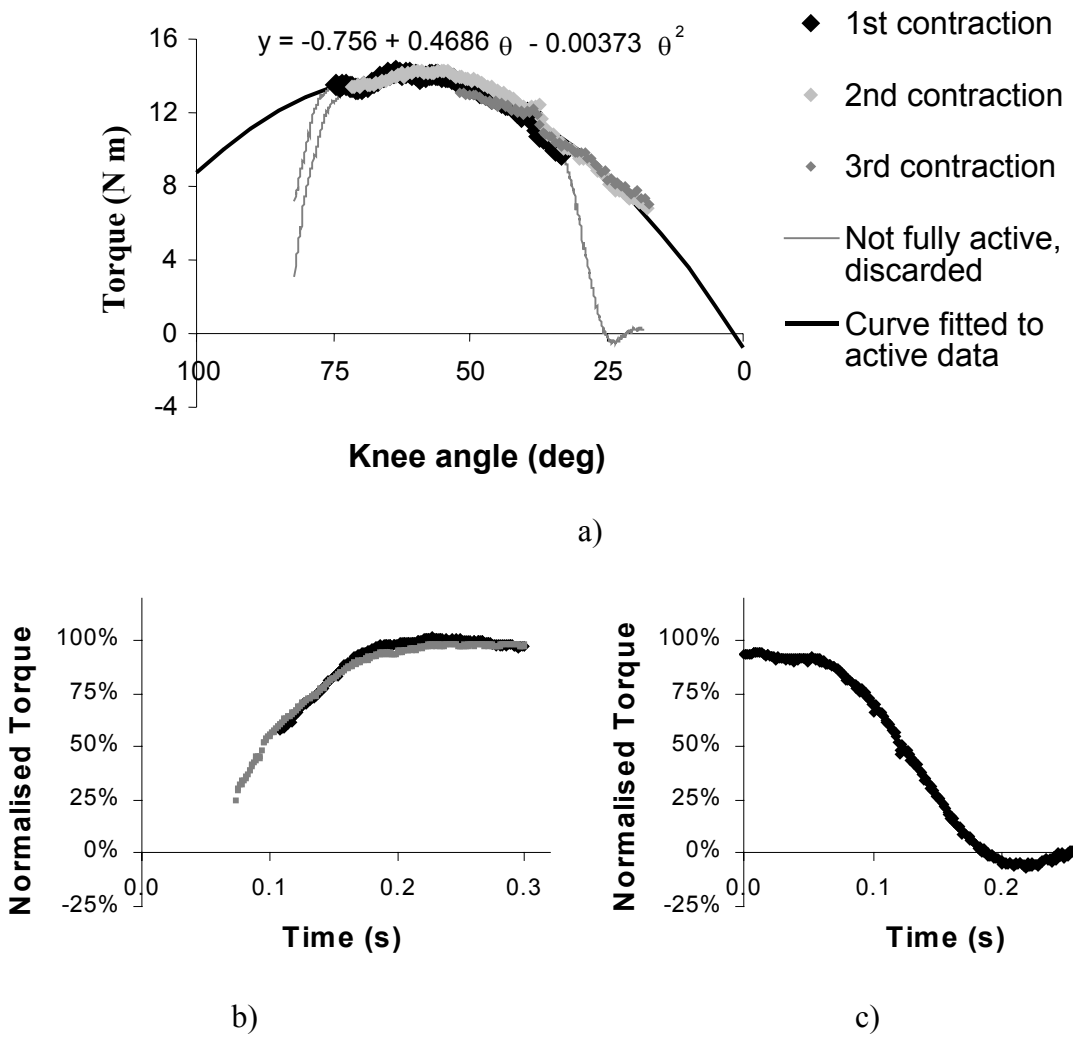

Figure 6.1.9.1 Illustration of the normalising procedure for dynamic contractions.

a) Three contractions within the one trial with different angles of stimulation onset and cessation. Only portions of each trial where angular velocity was constant have been shown. The quadratic curve was fitted to the fully active portions of the three contractions.

b) & c) Rise and fall periods have been normalised as a percentage of the quadratic curve fitted in part a). The time of each contraction has been adjusted so that stimulation commenced at time zero in a) and ceased at time zero in b). The two rising periods correspond to different knee angles because stimulation commenced at a different angle for each trial.

Figure 6.1.9.2 illustrates the mean activation rises calculated from all available contractions at each extension velocity. Much of the variation between velocities can be explained by different subjects being present at each velocity. For example, subject 3 produced slower rises than the other subjects for all velocities of contraction, but his results affect the 90 deg s^{-1} data more than other speeds because there are only two other subjects present at that speed. No trials for subject 3 were recorded at 120 deg s^{-1}, hence this velocity produced a greater mean rise rate than did 90 deg s^{-1}. Abrupt changes in the data series (eg 60 deg s^{-1}) result from the use of incomplete trials to boost numbers (eg Figure 6.1.9.1b). When one subject's data appears suddenly mid-way through activation, the mean can potentially jump because of the small numbers present.

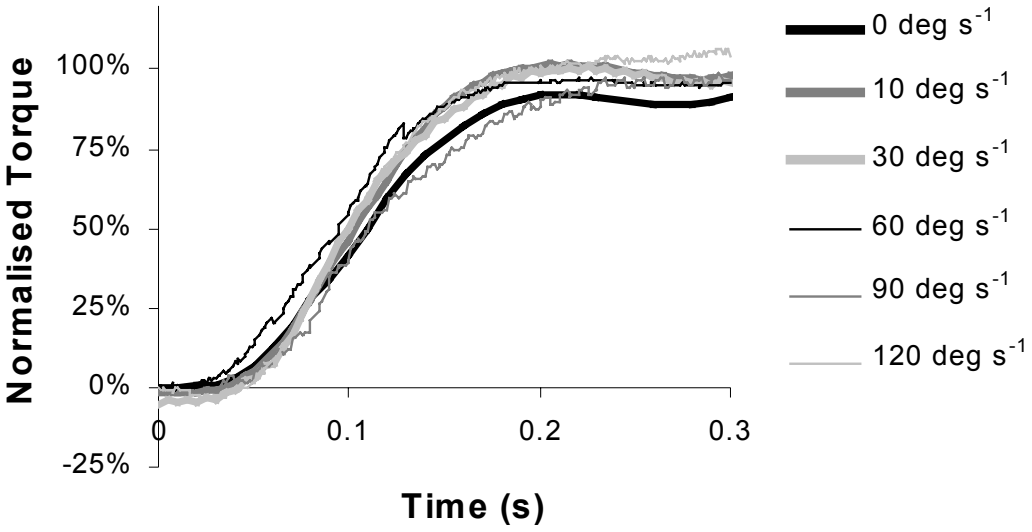

Figure 6.1.9.2 Normalised rises in torque averaged from all available trials at each velocity of knee extension.

The isometric trials appeared to demonstrate slower activation rises for all subjects while other velocities were more similar. The isometric results could not be attributed to skewing by individual subjects because all subjects were present at the slower speeds. While an error in the normalising process was suspected, a great deal of data checking was performed before the cause was isolated. Figure 6.1.9.3 illustrates normalised rise periods for isometric

contractions and slow isokinetic contractions as 10 deg s^{-1}. This figure shows a full second of following the onset of stimulation rather than the 0.3 s in Figure 6.1.9.2.

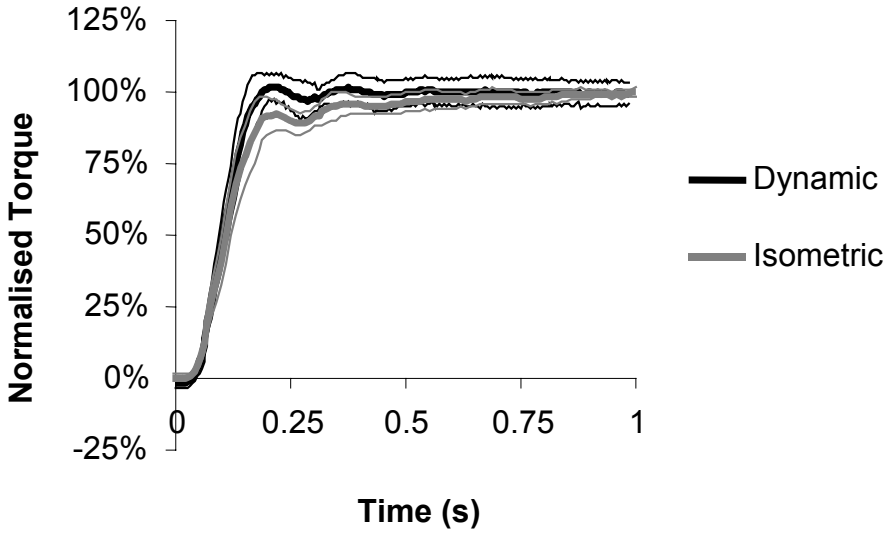

Figure 6.1.9.3 Comparison between normalised knee extension torque during isometric contractions and dynamic contractions at 10 deg s^{-1}.

There is a slow rise phase present throughout the plateau of most isometric trials so that 100% torque is not reached until after nearly one second. Collins et al. (2001) suggest that this slow rise during sustained contractions may result from the stimulation of low-threshold, afferent nerves; leading to the recruitment of additional motor units via a spinal reflex pathway. The slow rise phase is not present during the dynamic trials because, even if it occurred, the normalising process fitted a curve assuming activation was 100% after the initial rise period (see Figure 6.1.9.1). Looking at Figure 6.1.9.1, it would be impossible to distinguish between a slow plateau rise as demonstrated by isometric contractions and a rise caused by changes in fibre length and/or moment arm as the knee extended. The dynamic trials therefore rose quickly to 100% while the isometric trials took much longer to reach maximum torque.

Alternative methods were tried to improve the match between isometric and dynamic normalising processes. For example, the normalising process for isometric trials was changed

so that 100% torque was defined as the average value between 250 and 300 ms after stimulation, rather than the initial choice of 500 to 1500 ms. Figure 6.1.9.4 indicates that the alternative definition of 100% isometric torque resulted in a much better match between the rise phases of isometric and dynamic data. When the alternative isometric data was applied to Section 6.1.8, however, the model was no longer able to provide as close a match to the experimental data. It will be described below why the process of statistically comparing velocities was eventually abandoned, and the existing definition of 100% torque between 500 and 1500 ms after stimulation maintained.

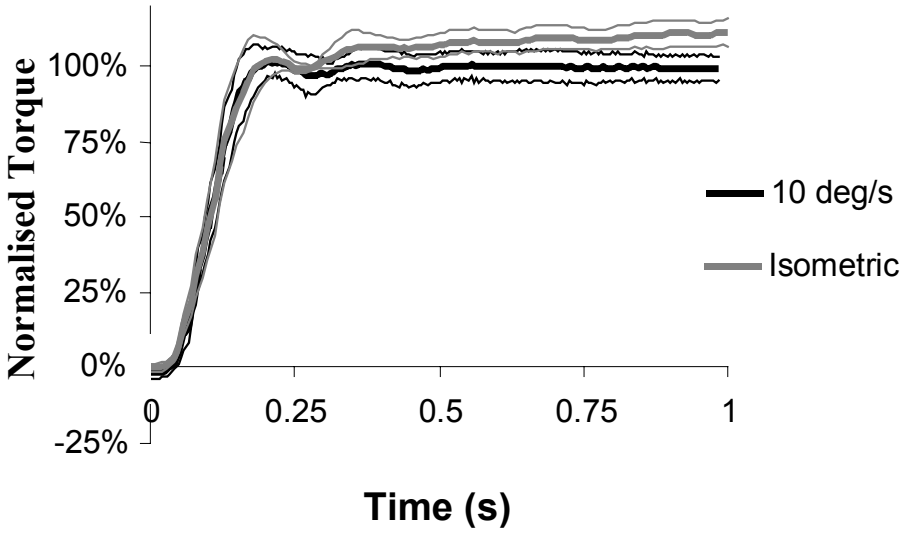

Figure 6.1.9.4 Comparison between isometric contractions and dynamic contractions at 10 deg s^{-1} using an alternative normalising procedure for isometric torque (see text for details).

If progress was to be made in analysing the rise data, then a statistical comparison had to be made between contractions. Preliminary tests assuming independent samples for each velocity suggested there were significant differences between velocities, but with no consistent pattern. For example, 90 deg s^{-1} rose more slowly than the others, 60 deg s^{-1} rose most quickly but 30 and 120 deg s^{-1} were very similar. Of course, these samples were not independent, because the same subjects were used across velocities. Different subjects, however, were often present at each velocity. Therefore, the differences between velocities could be

attributed to the subjects that were present at each velocity purely by chance. No repeated measures analysis could be performed because only one subject had contractions available at all velocities.

This must remain an area for further research. While it appears likely from Figure 6.1.9.2 that there was no change in activation dynamics with velocity of contraction, this cannot be demonstrated conclusively with the present data.

Figure 6.1.9.5 demonstrates the mean fall results for each velocity of contraction. Once again, these data are affected by small numbers; different subjects at each velocity and incomplete trials being used (Table 6.1.9.2). For example, 90 deg s^{-1} is very irregular because, although data from five subjects was available for the first 0.1 s, only one subject had data lasting the full 0.3 s for this velocity.

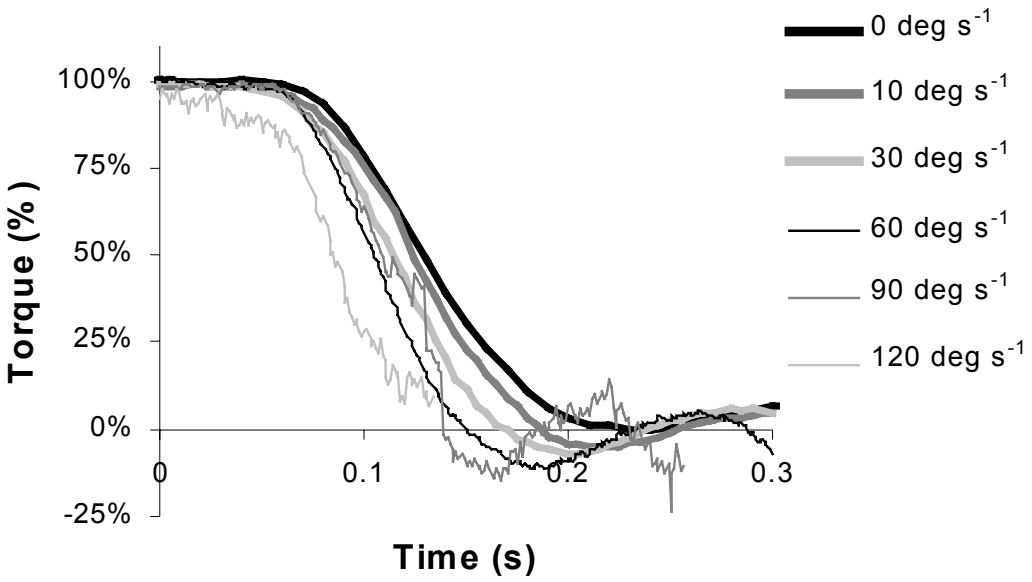

Figure 6.1.9.5 Normalised falls in torque averaged from all available trials at each velocity of knee extension.

Table 6.1.9.2 Number of fall periods available for analysis at each velocity of knee extension.

Velocity	Number of Contractions	Number of subjects
0	14	7
10	6	5
30	9	5
60	7	4
90	6	5
120	1	1
240	0	0

Because of the limited data set, the effect of contraction velocity on muscle relaxation will not be formally analysed here. The data do suggest a possible trend for decreasing relaxation times at higher velocities, because of the consistent pattern of change illustrated by Figure 6.1.9.5. Such a change could be speculated to result from increased viscous resistance at higher velocities reducing tension within the muscle. This finding, although not statistically testable, is consistent with results from Brown and Loeb (2000) that increased contraction velocity reduced muscle fall times after stimulation of feline caudofemoralis muscle. The velocity effect reported by Brown and Loeb was relatively small and inconsistent, particularly for stimulation frequencies closest to those used by the present study, and consequently they chose not to include this effect in their model of muscle activation dynamics. Similarly, the present model will also assume constant relaxation dynamics for all velocities of shortening.

6.1.10 Summary of fitting results.

- Parameters for tendon length were fitted to isometric data collected at different knee angles between 15 and 90 deg of flexion. The best fit for rectus femoris came from a tendon slack length of 0.351 m. For the vastii muscle, the fitted tendon length was 0.156 m.
- Fitting the model's muscle moment arms to isometric data at each knee angle was unable to improve predictions above those made using moment arms derived from Kellis and Baltzopoulos (1999).
- Similarly, fitting Hill constants to isokinetic results did not improve predictions above those made using constants reported by Pierrynowski and Morrison (1985).
- Activation constants for the rise and fall of joint torque in response to stimulation were fitted using isometric data collected at 60 deg. The resulting Rise Delay and Fall Delay constants were 53 and 66 ms respectively. The time constants for Rise Time and Fall Time were both 48 ms.
- It appears that activation parameters for the rise of torque remain constant across different joint velocities while relaxation may slow with increased angular velocity. The present data are not sufficient to demonstrate this conclusively; hence, values for isometric contractions will be used for all subsequent modelling.
- Muscle parameters such as moment arms, tendon lengths and Hill constants interact in complex ways. Therefore, great care must be taken when selecting values to ensure that parameters selected for one variable don't negatively impact on other components of the model. This is a major limitation of using fitting functions to obtain parameters, rather than measuring them directly.

6.2 Fitting model parameters to data from published literature

Tendon slack length was fitted to isometric knee extension data in Section 6.1.2 in order to match the joint angle predicted to produce maximum torque with the angle measured experimentally. In the absence of any experimental data for paralysed muscle contracting via NMES, previously published measurements for voluntary hip extension and knee flexion torque will be used to fit tendon lengths for the gluteus maximus and hamstring muscles within the present model.

6.2.1 Hamstring tendon slack length.

Normative data for knee flexion strength can be derived from work by Knapik et al. (1983). They measured maximum voluntary torque produced by male and female subjects at various speeds between 0 and 180 deg s^{-1} using a Cybex isokinetic dynamometer. While male subjects generated more torque than females, and isometric contractions generated more torque than dynamic ones, the general pattern of torque changes with angle were very similar for all conditions (Figure 6.2.1.1). Scudder (1980), also using a Cybex dynamometer, found similar patterns to those of Knapik et al. (1983). Hip angles were not reported by either study, however a photograph by Scudder (1980) shows an upright seating position with the hip flexed approximately 90 deg. It would be unlikely for Knapik et al. to have utilised a very different hip angle to this without reporting the angle.

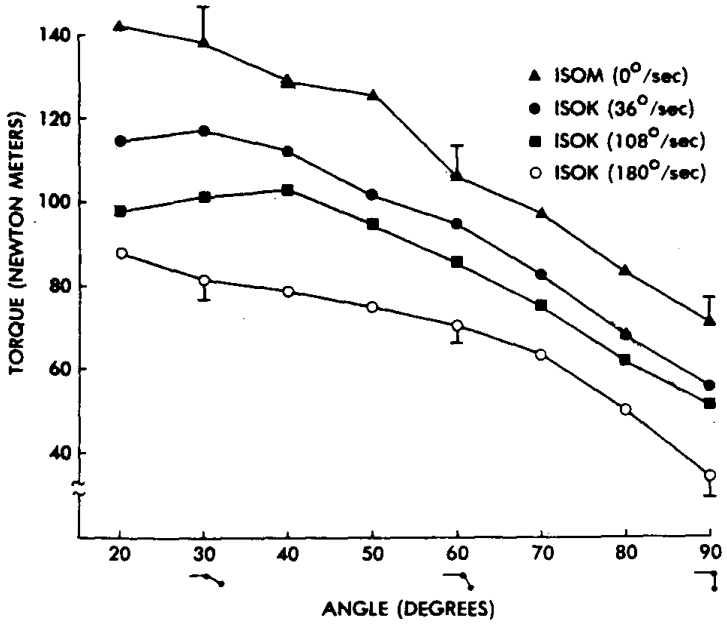

Fig. 3. Torque-joint angle curves for knee flexor muscles of the men.

Figure 6.2.1.1 Maximum voluntary knee flexor torque for males measured at various speeds of contraction. From Knapik et al. (1983), p941.

Similar methods to those of Section 6.1.2 were used to fit tendon slack lengths for the present model using isometric data from Knapik at al. (1983) and Scudder (1980). The hamstrings group, modelled as a single muscle with a tendon slack length of 0.385 m, predicted joint torques illustrated by Figure 6.2.1.2. This is the same slack length used by Hoy et al. (1990) using similar modelling methods, but slightly different moment arm and segment length parameters. It can be seen from Figure 6.2.1.2 that the model is quite sensitive to slack length, with only a 1 cm lengthening (approximately 2.6%) causing the modelled torque-angle curve to differ substantially from in-vivo measurements.

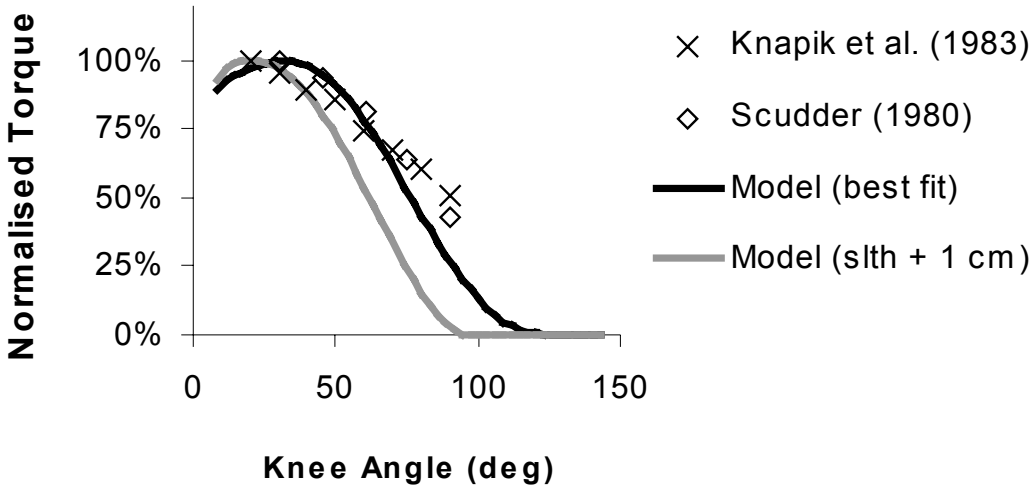

Figure 6.2.1.2 Comparison between knee flexion torque at different knee angles predicted by the model with those measured by Knapik et al. (1983) and Scudder (1980).

6.2.2 Gluteus maximus tendon slack length.

Waters et al. (1974) produced curves for hip extension strength in eight female subjects using a sciatic nerve block to limit the activity of the hamstring muscles during maximum voluntary hip extension contractions at various hip angles. Blocking the sciatic nerve reduced hip extension strength by approximately 50% at all hip angles, however the general shape of the torque-angle curve was similar to that produced without the nerve block (ie with hamstrings and adductor magnus assisting extension). As illustrated by Figure 6.2.2.1, the pattern of hip extension torque found by Waters et al. (1974) was quite similar to that measured subsequently by Nemeth et al. (1983) for maximum voluntary contractions using all hip extensors.

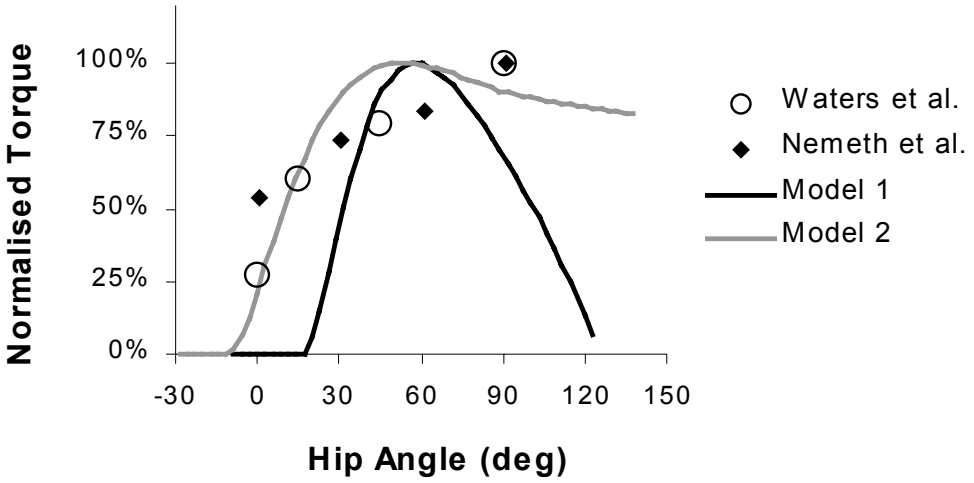

Figure 6.2.2.1 Comparison between hip extension torque at different hip angles predicted by three variations of the model with those measured by Nemeth et al. (1983) and Waters et al. (1974). Waters et al. (1974) measured hip extension torque from voluntary contractions by able bodied subjects; limited to gluteus maximus muscle by sciatic nerve blockage. Nemeth et al. (1983) measured hip extension torque from voluntary contractions of all hip extensors. Model 1 was calculated using gluteus maximus moment arms from Nemeth and Ohlsen (1985). Model 2 was calculated using gluteus maximus moment arms from Schutte (1992).

Modelled hip extension torque was initially compared to the published data using a gluteus maximus moment arm – hip angle function derived from Nemeth and Ohlsen (1985). This situation is labelled as "Model 1" in Figure 6.2.2.1. It can be seen that this single gluteal muscle was not able to generate torque over nearly as wide a range of hip angles as those measured through voluntary contractions. The gluteal model's single fibre was required to extend over lengths greater than the range through which active torque could be generated.

Model 2 was adopted using gluteus maximus moment arms adapted from Schutte (1992), rather than from Nemeth and Ohlsen (1985). Schutte modified a pre-existing model of musculo-skeletal geometry (SIMM, Delp et al., 1990) to include a cylindrical wrapping surface for gluteus maximus about the ischial tuberosity. This modification was necessary to cope with very flexed hip angles during cycling which would have otherwise have resulted in gluteus maximus passing through the ischium in a straight line muscle model. Although Schutte (1992, p136) states that her moment arm modelling is in agreement with Nemeth and

Ohlsen (1985), Figure 6.2.2.2 illustrates that her resulting moment arms are smaller, particularly as the hip approaches full extension. The advantage of using a smaller moment arm is that the gluteus maximus fibres are not required to change length to the same degree for a given range of hip flexion. Figure 6.2.2.1 illustrates that this allows the model to generate torque over a much wider range of hip angles than would otherwise be possible using moment arms derived from Nemeth and Ohlsen (1985). The tendon slack length fitted using Model 2 was 0.05 m; greater than the 0.001 m used by Hoy et al. (1990). The difference may have resulted either from different methods for determining gluteal moment arm or from a difference in the overall length of the muscle-tendon complex.

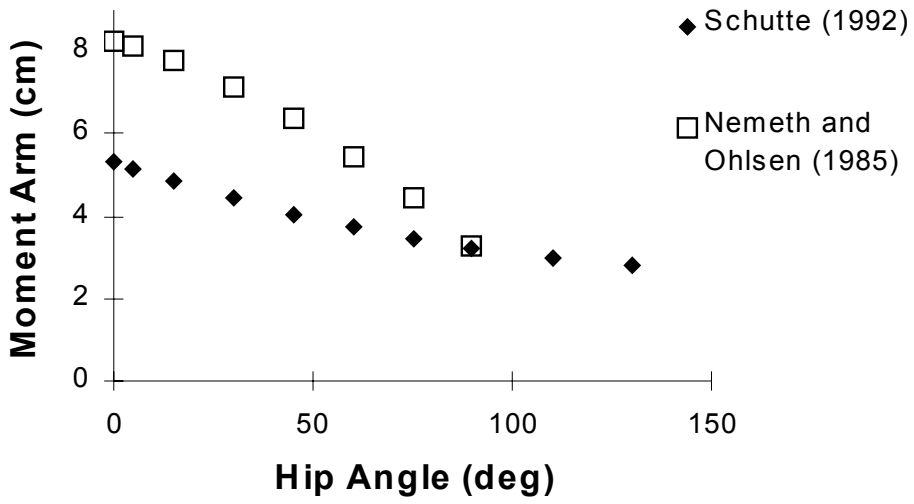

Figure 6.2.2.2 Comparison between gluteal moment arms reported by Nemeth and Ohlsen (1985) and those calculated by Schutte (1992).

Although model 2 demonstrates a closer match to the in-vivo data (Figure 6.2.2.1), modelled torque still cannot be generated over the range of hip angles measured during voluntary contractions. This result was also found by Hoy et al. (1990) using similar modelling methods. Schutte (1992), however, using a similar model to that of Hoy et al. and the present study, generated hip extension curves for gluteus maximus that matched the range of in-vivo values demonstrated in Figure 6.2.2.1. This wide range of angles over which extension torque was generated was produced using the same moment arms as the present study and a shorter fibre length. The torques produced by Schutte (1992) are therefore not likely to represent only

active force development within the muscle. Schutte used a parallel elastic element in her model, unlike that of Hoy et al. and the present study. Schutte's large extension torques at more flexed hip angles are therefore likely to represent tension in the muscle's passive elements, although no comment on relative contributions was made by Schutte. Unfortunately, there is no published data available on passive hip moments at very flexed positions. Available data does suggest, however, that there is little passive torque at hip angles up to 70 deg when the knee is flexed (Vrahas et al., 1990; Yoon and Mansour, 1982). While the parallel elastic component enabled Schutte's model to match the available in-vivo isometric data, passive movements and consequently the difference between active and passive movements would not be well modelled.

The active range of active torque development could be further increased by reducing moment arms further, but this option cannot be justified from present best estimates of moment arm length. Similarly, the model's fibre length could be increased further, but attempts to do this did not result in significant improvements of the model's match to experimental data. The failure to match modelled muscle forces to in-vivo data across a wide range of joint angles appears to be a problem inherent in trying to model a diverse muscle like gluteus maximus using a single fibre. To improve the model's performance, it would be necessary to model a number of fibres having different lengths and different moment arm functions. More anatomical measurements are required before this type of development could proceed further. For the present, this will be accepted as a limitation of the model and will be discussed further in Section 7.4.